Measurements of a Thermal-Conductivity Length Dependence in Helium II*

H. H. MADDEN, H. V. BOHM, M. D. COWAN, AND E. C. ALCARAZ
Department of Physics, Wayne State University, Detroit, Michigan
(Received 19 April 1965)

Helium II heat-flow measurements have been made in bundles of hollow glass fibers ($<10\,\mu$ in diameter) over the temperature range 1.5 to 2.1°K. A linear heat-current–versus–temperature-difference relationship was observed using channels 3, 6, and 9 cm in length. The experimental thermal conductivity varies approximately as T^{11} and decreases with increasing length of the channels; the latter result is apparently not accounted for by the theory of London and Zilsel. This length dependence is shown to be explainable in terms of a nonlinear temperature distribution along the channels. The consequence of this "length effect" on experimental determinations of normal fluid viscosity by heat-flow methods is briefly discussed.

I. INTRODUCTION

WHEN the heat-transport properties of helium II are measured, *a linear relationship between heat-current density and temperature gradient* is realized only when channels of very small size are used to contain the helium, and at the same time only small values of temperature gradient are allowed.[1–3] With these conditions satisfied, a coefficient of thermal conductivity can be defined and measured. Theoretical considerations based on the two-fluid model,[4] neglecting quadratic terms in the thermohydrodynamic equations of helium II and assuming perfect reversibility,[5,6] predict that the heat-current density for heat flow along the length of a cylindrical helium-II column of radius R is proportional to the temperature gradient along the column.[7] The coefficient-of-thermal-conductivity values resulting from this theory are solely dependent upon the radius R and the temperature T. An examination of early experiments[7] performed with helium II confined in small but very short channels suggested that the coefficient of thermal conductivity may actually depend on the length of the channel as well as on its radius and the temperature.

In 1958 Forstat[8] reported on a study of this length dependence. He used channels that were appreciably longer than those considered in the earlier examination and found a definite length dependence. This discrepancy between theory and experiment has received little attention in subsequent work, perhaps because of Forstat's use of a column of packed jeweler's rouge to obtain channels small enough for measurements to be made in the linear region; these have the obvious drawback of being extremely ill defined. Further, his subsequent analysis of the measurements was based on the oversimplifying assumption that such multiple-connected channels are equivalent to an array of parallel, noninterconnected, identical channels.

This paper reports on recent measurements of the dependence of the thermal conductivity of helium II on the length of the channels using parallel arrays of long, geometrically well-defined channels. The results show that the coefficient of thermal conductivity depends on the temperature roughly as predicted by theory, and also that the thermal conductivity does depend on the length of the channel. The latter result is not covered by present theoretical treatments.

II. DESCRIPTION OF THE CHANNELS

Our channels were fabricated by embedding hollow glass fibers, initially of 0.3-cm inside diameter, in a glass matrix.[9] Each unit comprises 1026 such fibers in a parallel array. These bundles of fibers were softened by heating and pulled down to form a continuous set of small, straight channels several meters in length. These long fiber bundles were then cut into 15-cm lengths and divided into three groups of equal numbers each consisting of an equivalent selection of cut lengths from various parts of the uncut bundles. The bundles in one of these groups were further cut into 9- and 6-cm lengths; those of the second group into 3- and 12-cm lengths; while those of the third group were left at their original cut length of 15 cm. Thus, groups of 3-, 6-, 9-, 12-, and 15-cm-length bundles having the same average channel size were obtained. (To date, only the 3-, 6-, and 9-cm lengths have been used in our experiments.) Finally, only those bundles for which all fiber orifices were circular in cross section and within a tolerance of $\pm 1\,\mu$ of the average (optically measured) channel diameter of $6.6\,\mu$ were retained for use in these measurements. The regularity of the fiber openings, in size and shape, is illustrated in Fig. 1.

Each experimental channel assembly was constructed by mounting seventeen capillary bundles in parallel between two stainless-steel header plates. The header plates were bonded to the capillary bundle ends using

* This research was supported by National Science Foundation Grants No. G-18808 and No. GP-1931.

[1] W. H. Keesom and G. Duyckaerts, Physica **13**, 153 (1947).
[2] J. H. Mellink, Physica **13**, 180 (1947).
[3] L. Meyer and J. H. Mellink, Physica **13**, 197 (1947).
[4] L. Tisza, Nature **141**, 913 (1938).
[5] L. Landau, J. Phys. USSR **5**, 71 (1941).
[6] R. B. Dingle, Proc. Phys. Soc. (London) **A62**, 648 (1949).
[7] F. London and P. R. Zilsel, Phys. Rev. **74**, 1148 (1948).
[8] H. Forstat, Phys. Rev. **111**, 1450 (1958).

[9] The hollow-fiber bundles were fabricated by the American Optical Company of Southbridge, Massachusetts.

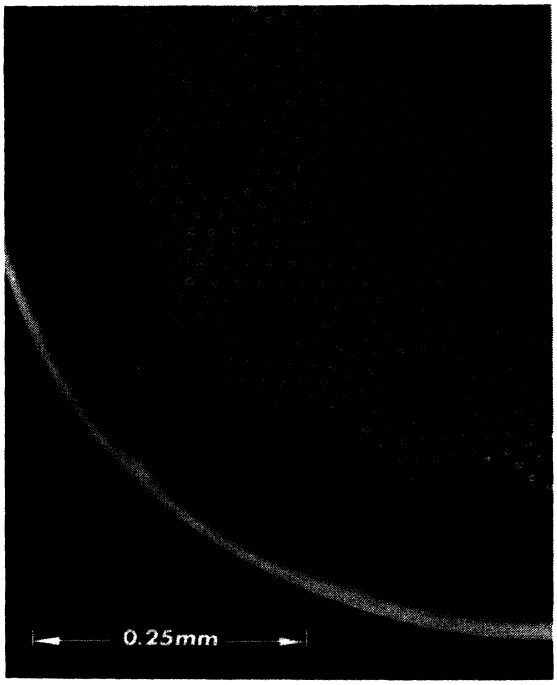

FIG. 1. Microphotograph (one-quarter view) of the end of a fiber bundle. The small dark spots are the capillary orifices. The light annular regions are the capillary walls and the darker region surrounding them is the embedding glass matrix. The outer boundary of the glass matrix is circular in cross section (diameter $\simeq$1.0 mm).

an epoxy resin[10] and were soldered to the brass components of the experimental chamber. Prior to a thermal-conductivity experiment, the channel assemblies were always tested for leaks in the solder joints and in the epoxy seals using a mass-spectrometric leak detector. Leak tests were made first at room temperature and were followed by tests during three or more temperature cyclings between room- and liquid-nitrogen temperatures. Finally the assembly was tested for superfluid leaks by immersing it in a liquid-helium bath and cooling below 2.0°K while the tightness of the assembly's joints was monitored with the leak detector.

III. APPARATUS AND PROCEDURE

Figure 2 shows schematically the part of the apparatus that was immersed in the liquid-helium bath during measurements. The channel assembly described above connected two liquid-helium reservoirs. The "hot" reservoir (HR), suspended from the lower end of the channel assembly in the vacuum region, contained a carbon-resistance thermometer ($\frac{1}{10}$ W, nominal 47-Ω Ohmite) and a Chromel-C wire-wound heater (2000 Ω). The leads to the thermometer and heater were fed out of this reservoir into the surrounding vacuum jacket through Stupakoff seals and from the vacuum region into the helium bath also through Stupakoff seals. Initially the remaining unoccupied volume in HR was about 3.5 cm^3. In recent experimental runs more than half of this dead space was filled with small glass beads in order to reduce the total heat capacity of HR by reducing the amount of liquid helium contained in it, and hence (1) to reduce the time required during the experiment for the system to come to an equilibrium temperature difference for a given heat input, and also (2) to reduce the time required for the system to reach a new equilibrium reference temperature (with no heat input) after a series of thermal-conductivity points had been taken at the previous reference temperature. For ease of exchanging channel assemblies of different lengths, the joint between the assembly and HR was made with low-melting-point (105°F) solder.

Low-melting-point (117°F) solder was also used to connect the channel assembly to the bottom of the "cold" (viz., reference temperature) reservoir (CR). This reservoir contained a carbon-resistance thermometer ($\frac{1}{2}$ W, nominal 47-Ω Ohmite), and a sensing thermometer and wire-wound heater that were connected to an electronic temperature regulator of the type designed by Sommers.[11] The electrical leads to these elements were fed out of CR to the bath through two 7-pin Winchester plugs. During the experiment the liquid helium contained in the experimental chamber was physically isolated from the bath liquid so that the quantity of helium in the experimental chamber re-

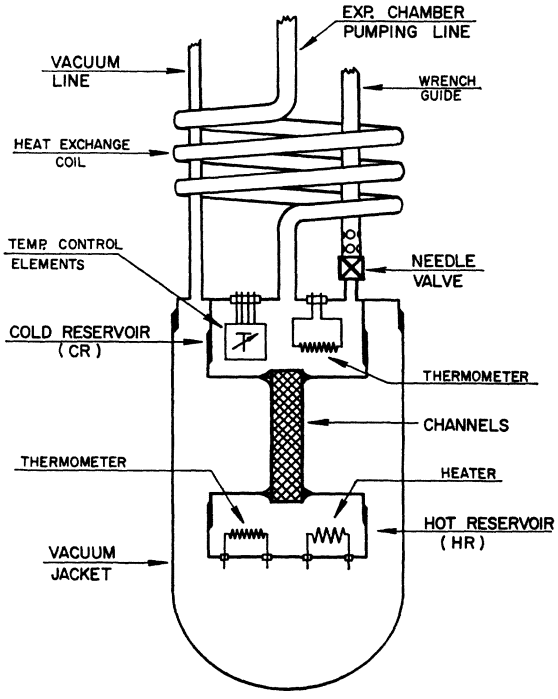

FIG. 2. Schematic of heat-flow apparatus.

[10] The best epoxy found for this operation was Minnesota Mining and Manufacturing Company's Structural Adhesive EC 2214.

[11] H. S. Sommers, Jr., Rev. Sci. Instr. **25**, 793 (1954).

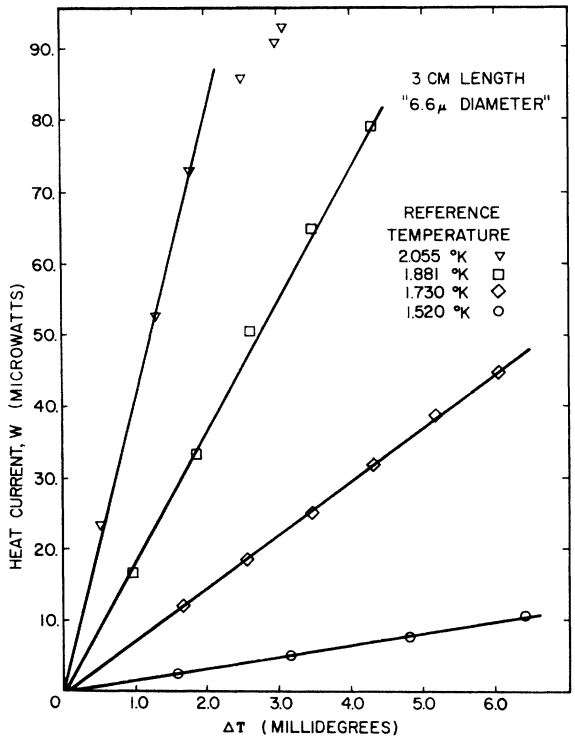

FIG. 3. Representative plots of total heat current versus temperature difference for a 3-cm-length assembly (run 51).

mained constant throughout the thermal-conductivity measurements. Heat supplied to the experimental chamber was carried to the helium bath by thermal conduction through the walls of CR. In order to enhance the thermal contact between the helium in CR and the bath helium, a heat-exchange coil was mounted in the experimental-chamber pumping line just above CR. The experimental chamber was filled from the helium bath through a needle valve (copper seat, phosphor-bronze plug) mounted in the top of CR and controllable from outside the cryostat by means of a long wrench.

HR and the channel assembly were surrounded by a vacuum region during the measurements. The glass vacuum jacket was sealed (housekeeper seal) to a short copper tube, which in turn was connected to a flange at the top of CR with low-melting-point (105°F) solder. This flange also contained the Stupakoff seals that fed electrical leads out of the vacuum region into the helium bath. The glass envelope of the vacuum jacket allowed a check to be made for clearance between HR and the inner wall of the vacuum jacket. After assembly of the apparatus this glass envelope was covered with aluminum foil to reduce stray radiation reaching HR.

Prior to the start of the actual experiment, the experimental chamber and the vacuum jacket were evacuated at room temperature to a pressure lower than 5×10^{-5} Torr. The vacuum jacket was then isolated and backfilled with helium exchange gas to a pressure of about 1 Torr, after which the apparatus was cooled, first overnight to liquid-nitrogen temperature, then to about 2°K, while continually pumping on the experimental chamber. The exchange gas was then pumped out of the vacuum jacket; next, the experimental chamber was isolated from the pumping system and filled with liquid helium from the bath through the needle valve. The needle valve was then reclosed.

A conventional (dc) four-lead, current-potential method was used to measure thermometer resistances and the energy input to the heater in HR. Two type-K-3 Leeds and Northrup, and a four-channel, type-4363D Guildline potentiometer were used in the measurements. For every thermal-conductivity point in our final data, a set of four or more heat input-temperature difference values were taken to ensure that measurements were restricted to the linear region of heat-conduction phenomena. Figure 3 shows typical plots, for a 3-cm length assembly, of heat current versus temperature difference for various reference (CR) temperatures. The 2.05°K (reference temperature) data in this figure show departure from straight-line behavior. Such nonlinearity (not intentionally looked for) was observed in our measurements only above ≈1.9°K and only with a 3-cm assembly; and even when it was observed, a linear portion of the data could always be discerned.

Values of the coefficient of thermal conductivity (K) were obtained by multiplying the slopes of straight-line plots of total rate of heat input versus temperature difference (e.g., Fig. 3) by the length of the channels and dividing by the total cross-sectional area of the channels, the latter computed as 17 bundles times 1026 capillaries per bundle times the cross-sectional area πR^2 of one capillary. An analysis of the amount of heat conducted by the glass and by the electrical (manganin) leads connecting HR and CR indicates that $<1\%$ of the heat was conducted along these paths even at the lowest temperatures reached in our measurements where K of the helium had its lowest values. For this reason the corrections for heat conducted by the glass and manganin have been neglected in the presentation of our data.

Immediately following each thermal-conductivity run the thermometers were calibrated against the vapor pressure of the helium isolated in the experimental chamber. A large-bore mercury-in-glass manometer, an oil (Octoil-S) manometer, and a Texas Instruments quartz-Bourdon gauge were used for the calibration measurements. Only after these calibration data were taken was the system again allowed to come to room temperature.

Several days of measurements were required to gather enough data to plot a K-versus-T experimental curve for a given length assembly. Further, it was found imperative to remove the liquid helium entirely from the experimental chamber at the conclusion of a run before the chamber warmed above the λ point; when this was not done, ruptures in the epoxy joints of the

channel assembly and/or in the solder joints of HR usually occurred. These ruptures were caused by the inability of He I to escape HR sufficiently rapidly through the capillaries as HR temperature rose toward the critical temperature. Thus, the temperature of the helium bath was continuously held below the λ point, and, using a device especially designed for transfer of 4.2°K liquid into a below-λ region,[12] new liquid was added daily to the bath.

IV. RESULTS AND ANALYSIS

Measurements were initially made on three assemblies indentically constructed except for a difference in their lengths (runs 50, 51, and 52). The experimental data were first analyzed with the assumptions that all three assemblies had the same number of open channels (17 times 1026), and that all channels were identical in diameter (6.6 μ), and uniform along their lengths. These assumptions seemed to be justified on the basis of the uniformity in size and shape of the channels observed in optical measurements on the cut ends of the capillary bundles (Fig. 1) and the precautions noted in Sec. II. The results[13] presented in Fig. 4 and in Table I show

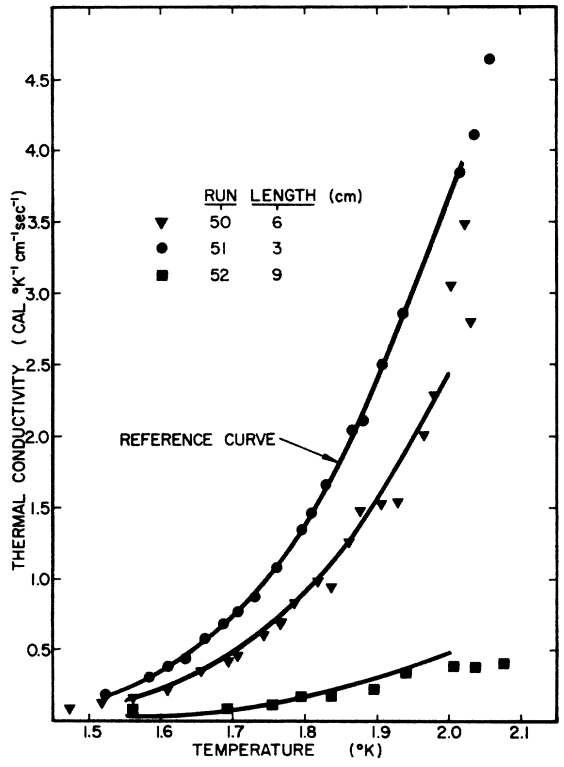

FIG. 4. Thermal conductivity as a function of temperature for three different length assemblies; data shown does not include gas-flow measurement corrections.

[12] H. H. Madden and H. V. Bohm, Rev. Sci. Instr. 35, 1554 (1964).

[13] H. H. Madden, R. H. Hammerle, and H. V. Bohm, *Proceedings of the Ninth International Conference on Low Temperature Physics, 1964* (Plenum Press, Inc., New York, to be published).

TABLE I. Thermal-conductivity data; maximum superfluid velocities attained during measurement of the thermal-conductivity value.

Run identification	T (°K)	K_{expt} $\left(\frac{\text{cal}}{\text{°K cm sec}}\right)$	v_s (cm/sec)
	1.520	0.187	0.020
	1.583	0.304	0.021
	1.609	0.391	0.019
	1.634	0.449	0.055
	1.660	0.579	0.046
	1.684	0.688	0.094
	1.706	0.772	0.063
	1.730	0.877	0.10
$L=3$ cm	1.760	1.078	0.035
Run No. 51	1.795	1.345	0.18
Assembly No. L3A	1.809	1.469	0.074
	1.828	1.664	0.18
	1.865	2.049	0.11
	1.881	2.102	0.21
	1.907	2.507	0.11[a]
	1.936	2.852	0.25[a]
	2.015	3.843	0.35[a]
	2.035	4.105	0.38[a]
	2.056	4.647	0.31[a]
	1.470	0.0917	0.008
	1.516	0.125	0.021
	1.560	0.172	0.022
	1.607	0.224	0.013
	1.655	0.356	0.031
	1.692	0.425	0.027
	1.706	0.463	0.026
	1.740	0.603	0.046
	1.765	0.693	0.039
$L=6$ cm	1.785	0.829	0.056
Run No. 50	1.816	0.992	0.068
Assembly No. L6A	1.836	0.945	0.059
	1.860	1.258	0.080
	1.876	1.482	0.069
	1.905	1.530	0.065
	1.928	1.537	0.072
	1.965	2.012	0.12
	1.981	2.251	0.12
	2.002	3.052	0.17
	2.021	3.494	0.037
	2.031	2.720	0.18
	1.560	0.0819	0.058
	1.692	0.0865	0.0093
	1.754	0.117	0.021
$L=9$ cm	1.794	0.173	0.016
Run No. 52	1.837	0.180	0.027
Assembly No. L9A	1.896	0.232	0.017
	1.940	0.334	0.029
	2.005	0.394	0.070
	2.036	0.388	0.025
	2.077	0.412	0.050

[a] Departures from linearity observed; v_s value given corresponds to the greatest value for points in the linear range.

a sizeable "length effect" with K decreasing with increasing length of the channels.

One possible explanation for the results shown in Fig. 4 was that clogging of the longer channels had occurred due to freezing out of condensible vapors. On the basis of this hypothesis the results would be due to insufficient (room-temperature) pumping time being allowed, before the start of an experiment, for HR and the channels to be thoroughly cleansed of condensable vapors. This hypothesis was tested and shown to be incorrect by repeat measurements (runs 53 and 54)

made on the same 9-cm channel assembly used in run 52. Following run 52, two weeks were spent at room temperature in flushing the experimental chamber with dry helium gas, and in extensive pumping on this chamber between the flushings before the start of run 53. Between runs 53 and 54 a similar clean-up procedure was carried out over a one-month period. The results of runs 53 and 54 do not differ significantly from those of run 52. In the remaining analysis given below, these three runs are treated as one.

In order to check the reproducibility of the results, measurements were next made on a different 3-cm and a different 6-cm assembly (runs 56 and 57) from those used in runs 51 and 50, respectively. The data from runs 56 and 57, analyzed as outlined above do not agree with those of runs 51 and 50. This discrepancy suggested that the optical measurements showing channel uniformity at their ends were insufficient evidence to justify the assumption that the channels were uniform to hydraulic flow. A series of room-temperature helium-gas-flow measurements made on all five channel assemblies used in the thermal-conductivity measurements showed that the total cross-sectional areas open to flow were not the same for all assemblies. The thermal-conductivity results had thus to be re-evaluated on the basis of these gas-flow measurements.

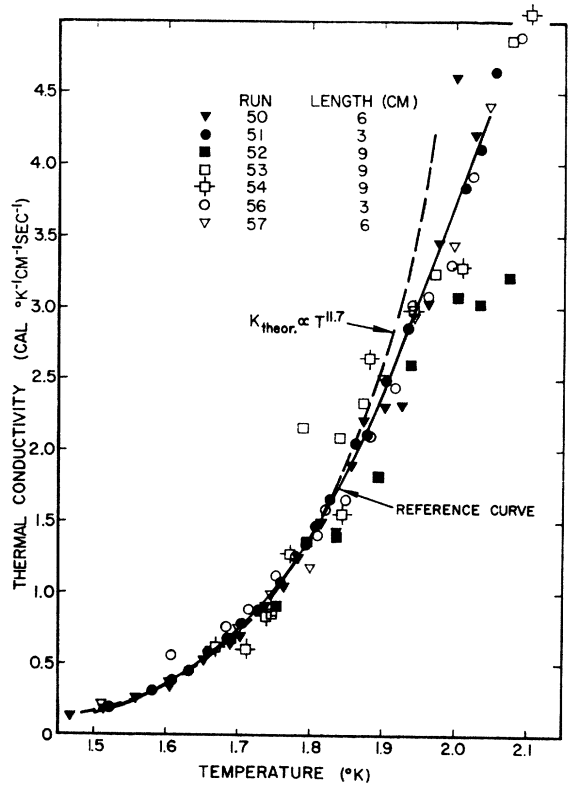

FIG. 5. Thermal conductivity as a function of temperature for seven runs on assemblies of three different lengths normalized to reference run 51.

TABLE II. Uncorrected and corrected thermal-conductivity ratios; channel-geometry parameters.

(1) Run Number	51 (Reference)	56	50	57	52, 53, and 54 (Composite)
(2) Assembly	L3A	L3B	L6A	L6B	L9
(3) Length (cm)	3	3	6	6	9
(4) Uncorrected thermal-conductivity ratio (κ)	1.0	0.87	0.66	1.03	0.13
(5) Measured gas-flow rate ratio (ϕ)	1.0	1.08	2.52	1.68	13.4
(6) Average-areas ratio (α)	1.0	0.96	0.89	1.09	0.47
(7) Channel-numbers ratio (ν)	1.0	0.93	0.79	1.19	0.22
(8) Corrected thermal-conductivity ratio (κ')	1.0	0.94	0.83	0.87	0.58

Without reference to the gas-flow measurements, it is of interest to examine the values of K obtained from the various runs for similarities in their temperature dependence. The data can be made to fall approximately on one curve of K_{expt} versus T by scaling each run by a constant factor appropriate for that run. Run 51 (the first 3-cm-length assembly run) was taken as a reference since the data from this run were the best defined of all the runs. Scaled data from all seven runs are plotted in Fig. 5. In order to determine a scaling factor for a given run, a scaling factor for each data point of the run was determined and an average scaling factor calculated for the run. Values of κ, the reciprocal of the average scaling factor, are tabulated in line 4 of Table II. The individual scaling factors for the 9-cm-length assembly points above 2.0°K were markedly larger than those for the points below that temperature; they were not used in calculating the average scaling factor for the 9-cm data (runs 52, 53, and 54). Except for these points, the scaled data are internally consistent in their general temperature dependence. The 9-cm-length assembly data suggest the possibility of a maximum in the experimental K-versus-T curves.

The results of the room-temperature gas-flow measurements are given in line 5 of Table II in terms of ϕ; this quantity is defined as the ratio[14] of the volume rate of flow through channel assembly L3A (the assembly used in reference run 51) to the volume rate of flow through another given channel assembly. The gas-flow measurements were all carried out in the same pressure range and under conditions where flow is governed by Poiseuille's equation. The Reynolds numbers calculated for the gas-flow experiments were $<10^{-4}$. The expected values for ϕ (on the basis of identical channel size and number) were simply $\phi=L/(3\text{ cm})$. The differences between the expected and measured values of ϕ were interpreted on the basis of two alternate premises. The first is that there existed differences in the average-radius values between channel assemblies; these differences are given in line 6 of Table II in terms of α, the ratio of the average area of channels in a particular channel assembly to the average area of channels in the reference assembly. The alternate

[14] Comparative ratios are given Greek-letter symbols in this paper.

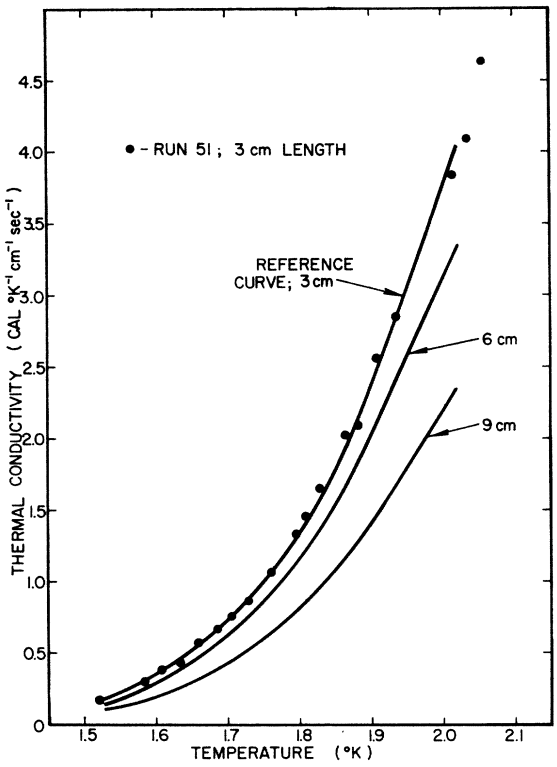

FIG. 6. Thermal conductivity as a function of temperature for three different length assemblies; curves are corrected to account for gas-flow measurements.

premise is that different assemblies had different numbers of open channels; these differences are given in line 7 of Table II in terms of ν, the ratio of the number of channels in a channel assembly to the number of channels in the reference assembly.

The values of κ tabulated in line 4 of Table II, and previously referred to as the reciprocals of the average scaling factors, are uncorrected ratios (with respect to the gas-flow measurements) of the thermal conductivities of channels of length L, to the thermal conductivity of the reference channel. The values of κ correspond to a "length effect" of the magnitude shown in Fig. 4. Recalculated values of the thermal-conductivity ratios (κ') are tabulated in line 8 of Table II; both above premises lead to the same reduced thermal-conductivity ratios. (See Appendix for details.) The recalculated ratios show a "length effect" in the direction originally observed but smaller in magnitude. This is illustrated in Fig. 6.

The "length effect" is not evident in current theoretical results. From the linear thermohydrodynamic equations of motion[5] for the two-fluid model of helium II, London and Zilsel[7] obtain a theoretical expression for K (for the case of heat flow along a cylindrical column of helium II):

$$K=(\rho S)^2TR^2/8\eta_n, \tag{1}$$

where ρ is the mass density, S is the specific entropy of the liquid, η_n is the coefficient of viscosity of the normal component of helium II, R is the radius of the liquid column, and T is the absolute temperature of the liquid. Using the empirical result that the entropy density (ρS) of helium II varies approximately as $T^{5.6}$ in the temperature range from 1°K to the λ point, and assuming that "$\eta_n \propto T^{0.5}$, as is the case in an ideal gas and in helium I,"[7] they predict a temperature dependence (R constant) of $K \propto T^{11.7}$.

Equation (1) is derived for conditions of zero net mass transfer, steady-state hydrodynamic flow, and no viscous dissipation of energy. Our experimental system fully satisfies the first two conditions; as will be discussed below, any viscous dissipation occurring has apparently a negligible effect on our results. Using the value of the channel radius as the fitting parameter, a theoretical curve $\propto T^{11.7}$ has been fitted to the 3-cm (reference) data in Fig. 5. A value of $R \approx 0.8\ \mu$ gives the best fit to the experimental points. K_{expt} does not increase quite as fast with temperature as the theory predicts (indeed, a plot of $\log_{10}K_{\text{expt}}$ versus $\log_{10}T$ gives a power of 11.0). The difference in value between the theoretical fitting parameter R of 0.8 μ and the optically measured radius of 3.3 μ may be related to the discrepancies between the optical and the hydraulic-flow measurements of channel size and uniformity. It should also be noted that if one knew how to extrapolate the 3-cm (reference) K_{expt} to a "zero-length" value, the fitting parameter R would be nearer the optically measured radius.

Possible phenomenological explanations of the experimental results are considered next. For a linear temperature distribution the temperature difference between the ends of a channel divided by the length of the channel is constant for any length channel. If however, the temperature distribution along the channel were nonlinear, in particular if it were of the shape illustrated in Fig. 7, the experimentally determined temperature gradients for 3-, 6-, and 9-cm-length assemblies would correspond to the slopes, $(T-T_0)/L$, of the chords 0-3, 0-6, 0-9, and would thus not be equal. Such a nonlinear temperature gradient would be in agreement with the apparent dependence of K_{expt} on the length of the channel. As a representative nonlinear temperature distribution, a power law

$$T=T_0+(dT/dL)_0[L+BL^p] \tag{2}$$

was tried in analyzing our data. In Eq. (2), T_0 is the temperature at CR, L is the distance along the channels measured from CR, $(dT/dL)_0$ is the initial slope at $L=0$, and B and p are constants to be determined from a comparison with experimental results. Thus, in terms of this temperature distribution the slopes of the chords in Fig. 7 are

$$(T-T_0)/L=(dT/dL)_0[1+BL^{p-1}]. \tag{3}$$

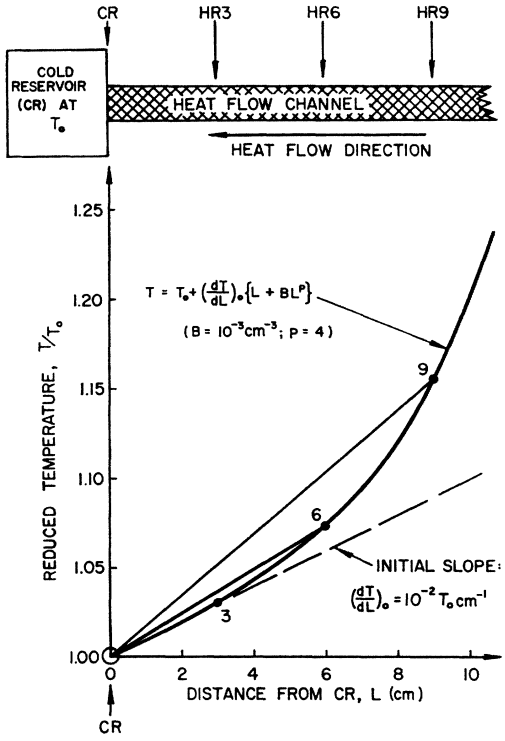

FIG. 7. Hypothetical plot of temperature distribution in a channel as a function of distance along the channel from the cold reservoir (fixed at temperature T_0).

Representative values of B and p (calculated using κ' values from line 8 of Table II for run 50 and the composite 9-cm run) are $B=1.5\times10^{-3}$ (in units of $cm^{-2.9}$), and $p=3.9$; both have a strong dependence on the magnitude of the "length effect." Since K_{expt} decreases with increasing L, we have $B>0$ and $p>1$ as necessary conditions. Thus any nonlinear temperature distribution must have an increasing slope as illustrated in Fig. 7.

The initial slope $(dT/dL)_0$ should be obtainable from the limiting value of the thermal conductivity as L goes to zero:

$$\lim_{L\to 0} K(L) = K_0 = \frac{(W/A)}{(dT/dL)_0}, \tag{4}$$

where W is the total heat input per unit time, and A is the total cross-sectional area of the channels. Attempts to extrapolate the corrected K_{expt} values to a "zero-length" value have been made, but an explicit expression for the dependence of K_{expt} on the length of the channels that fits all data could not be determined.

In the above analysis it has been assumed that the heat-current density (conventionally defined, for purposes of calculating experimental data, as the ratio of the measured heat input at HR to the cross-sectional area of the channels) is constant along the entire length of the channels. If it is assumed that K is truly independent of length, but that heat-current density (J) changes along the channels are responsible for the nonlinear temperature distribution illustrated in Fig. 7, an alternate analysis can be developed. A changing J might be due to heat created or lost along the channels or to a changing effective cross-sectional area through which the heat flows.

Heat is generated in the flow of the viscous normal fluid from HR to CR. It produces an increasing J as one goes from HR to CR. This contribution to the heat flow is among the nonlinear terms neglected by London and Zilsel as insignificantly small in the derivation of Eq. (1). The steadily increasing slope of the curve in Fig. 7 as one goes from CR to HR requires a *decreasing* J as the heat flows from HR to CR. Heat losses by conduction or convection were prevented by the vacuum surrounding the channels. Heat losses by radiation have been calculated to be too small to account for the observed "length effect"; the temperature differences between the walls of the capillaries and the helium bath surrounding the aluminum-foil shielded vacuum jacket were less than 0.01°K.

An increase in the average effective cross-sectional area of the channels as the heat flows from HR to CR would yield a decreasing J. Such a consistent variation in geometrical area can hardly be expected for all five channel assemblies; however, changes in the normal fluid velocity profile along the length of the channel could result in a variation in effective area. It must be noted that "end effects" which are usually associated with a changing velocity profile, appear to be negligible. The maximum Reynolds Numbers, $M=2Rv_n\rho_n/\eta_n$, for the normal fluid flow are of the order of 3, and thus the inlet lengths, defined[15] as $0.07RM$, are less than 10^{-4} cm.

V. DISCUSSION

At the start of this research project we were very skeptical about the existence of a "length effect" as suggested by London and Zilsel[7] and reported by Forstat.[8] London and Zilsel arrived at the possibility from a consideration of two independent experiments,[1,3] in both of which the channels used were very short ($\approx$0.1 to 0.3 cm in length), in each of which a channel of one length only was used, and in one of which the establishment of steady-state conditions during measurements was questionable. Forstat's model of a set of parallel, noninterconnected channels, all of the same length, shape, and size does not agree well with the real channels through a column of packed jeweler's rouge. In applying the laws of hydrodynamics to the flow of normal fluids through porous media one must make a number of simplifying assumptions, and even when more realistic models than that assumed by Forstat are used, the flow of normal fluids through porous plugs exhibits deviations from Poiseulle's law.[16] Clearly,

[15] R. B. Bird, W. E. Stewart, and E. N. Lightfoot, *Transport Phenomena* (John Wiley & Sons, Inc., New York, 1960), p. 47.
[16] P. Debye and R. L. Cleland, J. Appl. Phys. **30**, 843 (1959).

simplifying assumptions must be examined carefully in dealing with helium II. Further, Reynolds and co-workers,[17] using an experimental setup similar to that used by Forstat,[18] reported results that appear to show a "length effect" in the opposite direction to that reported by Forstat.[8]

Section IV deals first with reducing the magnitude of the "length effect" to a value consistent with the gas-flow measurements. Of the limiting hypotheses considered, average channel-radius differences are the least credible situation since the capillary fabrication, cutting, and selection methods discussed in Sec. II make variations (systematic or otherwise) in capillary size of sufficient magnitude to explain the gas-flow discrepancies improbable. Total capillary number differences, due to clogging, are the more probable situation since optical measurements, while showing no evidence of clogging or capillary collapse, could be made only on the ends of the capillary bundles. Clogging for a short distance anywhere along the length of the channels would effectively remove the channel as an "internal convection" path. Neither of the extreme cases leads to an elimination of the "length effect." Analyses of intermediate cases, i.e., combinations of differences in area and of clogging that satisfy the gas-flow results, are more difficult to carry through, but in any case do not appear to lead to the elimination of the "length effect."

Our interpretation of the "length effect" on the basis of a nonlinear temperature distribution does not lead to a clear-cut explanation of why K should change as it appears to when J is taken as constant along the channels, or, alternately, why J should change, as it must, if K is taken as constant along the channel. Suspect then is the validity, for the case of a helium II column of finite length, of the theoretical expression for K given in Eq. (1). Equation (1) is derived for differential temperatures and lengths. Perhaps if the London-Zilsel differential thermohydrodynamic equations were properly integrated with respect to both length and temperature, a length dependence of K would result.

The validity of Eq. (1) under the above conditions may be further questioned by considering experimental determinations of η_n by heat-flow methods.[17,19–21] The evaluation of K given by Eq. (1) is crucial in such experiments. If K decreases with increasing length of the channel through which the heat (normal fluid) flows, the values of η_n calculated using K determined by Eq. (1), which does not include a length dependence, will be larger than "actual," though the "actual" experimental values are not definitely established.[22–24] Ordinarily, η_n-heat-flow experiments employ very small slits[19] or capillaries[20] to avoid nonlinear heat-flow phenomena; hence, data reduction involves the formidable difficulties of ascertaining exact flow geometries of these narrow channels. Staas and co-workers[21] have performed experiments using "wide" capillaries that were carefully calibrated for channel size and uniformity using a "mercury drop" method, rather than the more conventional, but less accurate, gas-flow method.[17,19,20] Their elegant technique apparently avoided the nonlinear effects usually seen in wide channels. Below 1.7°K, they obtained results in agreement with the rotating-cylinder viscometer results of Heikkila and Hollis Hallet.[23] Above this temperature their η_n values are larger than those measured by the rotating-cylinder method. This difference is consistent with the "length effect," its absolute magnitude becomes smaller, the lower the temperature. This might be expected because of the rapid decrease in K with temperature and the resultant insensitivity of η_n calculations to small changes in K.

A number of further experiments are suggested by the work reported here. A check on the linearity of the temperature distribution along the channels would be valuable. Also desirable would be a series of experiments on the "length effect" using channels that may be broken into sublengths in such a way that none of the original channels is lost in the subdividing process, as would necessarily have occurred with our 17-bundle capillary assemblies. Such studies would eliminate the need for corrections for channel size- and number-differences and thus remove the aspect of our experimental results that makes the exact dependence of K on the length of the channels difficult to determine. Finally, independent of the "length effect," measurements of K should be made as T approaches the λ point in order to determine under what conditions, if any, a maximum occurs in the K_{expt}-versus-T curve, as reported by Forstat[8] and as suggested by our 9-cm-length data.

ACKNOWLEDGMENTS

Apart from the financial support of the National Science Foundation, gratefully acknowledged in the footnote to the title, some financial help was received from the University of Michigan Institute of Science and Technology during the initial construction stages of this work.

The authors especially wish to thank Dr. Richard F. Woodcock of the American Optical Company, whose continuing interest and patience made possible the successful fabrication of our fiber bundles.

[17] J. Burnham, J. Reppy, G. Pearson, A. H. Spees, and C. A. Reynolds, Phys. Fluids 3, 735 (1960); (cf. Fig. 2 of that paper).

[18] H. Forstat and C. A. Reynolds, Phys. Rev. 101, 513 (1956).

[19] A. Broese Van Groenou, J. D. Poll, A. M. G. Delsing, and C. J. Gorter, Physica 22, 905 (1956).

[20] D. F. Brewer and D. O. Edwards, Proc. Roy. Soc. (London) A251, 247 (1959).

[21] F. A. Staas, K. W. Taconis, and W. M. Van Alphen, Physica 27, 893 (1961).

[22] E. Andronikashvili, Zh. Eksperim. i Teor. Fiz. 18, 429 (1948).

[23] W. J. Heikkila and A. C. Hollis Hallett, Can. J. Phys. 33, 420 (1955).

[24] K. M. Eisele and A. C. Hollis Hallett, Can. J. Phys. 36, 25 (1958).

Since the start of this project more than a dozen undergraduates have, at various times, aided in construction, data taking, and data reduction; almost all were participants in the National Science Foundation sponsored Undergraduate Research Participation Program operated at the Wayne State University Physics Research Laboratory. Among these students, we are particularly indebted to R. H. Hammerle, J. L. Smith, and A. G. Cohen. Hammerle continued working on the project as a graduate student, as part of his work in fulfilling the requirements for the Master of Science degree. Another graduate student, J. D. McNutt, contributed substantially to the construction of the cryogenic system. It is a pleasure to acknowledge the skilled apparatus construction by John VanGemmen and his colleagues in the Research Laboratory shop.

APPENDIX

Reduction of the uncorrected thermal-conductivity ratios[14] κ in light of the gas-flow results is based, in both the average-radius differences and clogging limits, on Poiseulle's equation for the volume rate of flow F of a gas of viscosity η through N identical cylindrical capillaries of radius R and length L:

$$F=N\pi(\Delta p)R^4/8\eta L, \tag{A1}$$

where Δp is the pressure difference between the ends of the capillaries. Measurements of F could not be made with sufficient accuracy to determine absolute channel sizes. Rates of pressure change in the constant-volume gas supply chamber used in all gas-flow measurements were measured accurately, and, taking these rates as proportional to the F values, an accurate ratio ϕ of F for the reference assembly to F for any other assembly was determined. If each assembly has the same number N of identical channels of radius R, from Eq. (A1) this ratio is

$$\phi=L/(\text{reference length})=L/3\text{ cm}. \tag{A2}$$

Experimental conditions were such that η and Δp were the same for each gas-flow measurement. Differences between the expected and measured values of ϕ could only be due to (i) differences in R, (ii) differences in N, or (iii) a combination of differences in R and N. From a single set of gas-flow measurements a definite choice among these possibilities cannot be made. Thus, the two extremes, (i) and (ii), were considered separately.

Case (*i*). Reduction for average-radius differences (κ_a): In this limit N is the same for all channel assemblies ($=N_r$), but the average channel radius of the reference assembly R_r is not necessarily the same as that of any other assembly R_L. Thus

$$\phi=[L/(3\text{ cm})](R_r/R_L)^4, \tag{A3}$$

or the average-areas ratio is

$$\alpha=\frac{\pi(R_L)^2}{\pi(R_r)^2}=\left(\frac{R_L}{R_r}\right)^2=\left[\frac{L/(3\text{ cm})}{\phi}\right]^{1/2}. \tag{A4}$$

Initially, K_{expt} values were calculated according to

$$K_{\text{expt}}=\frac{W/(N_r\pi R_r^2)}{\text{grad}T}, \tag{A5}$$

where W is the measured rate of heat input to HR, and grad T is the measured "temperature gradient" (Fig. 7). To correct K_{expt} in this limit, R_r^2 must be replaced by R_L^2, thus giving a new K_{expt}' allowing for area differences,

$$K_{\text{expt}}'=K_{\text{expt}}\left(\frac{R_r}{R_L}\right)^2=\frac{K_{\text{expt}}}{\alpha}. \tag{A6}$$

The theoretical K depends on the square of the radius of the channel:

$$K_{\text{th}}=\text{constant}\times R^2T^{11.7}. \tag{A7}$$

Thus K_{expt}' should be compared with a new reference curve that corresponds to experimental results for a 3-cm assembly with an average radius R_L instead of R_r. From Eq. (A7), this new curve is obtained by multiplying the original reference curve K_r, shown in Fig. 5, by α. The thermal-conductivity ratio κ_a, corrected for area differences, is then

$$\kappa_a=\frac{K_{\text{expt}}'}{K_r\alpha}=\frac{K_{\text{expt}}/\alpha}{K_r\alpha}=\frac{\kappa}{\alpha^2}. \tag{A8}$$

Case (*ii*). Reduction for number differences (κ_n): Assuming R is the same for all channels ($=R_r$), the difference in total cross-sectional area of the channels reflected in the measured gas-flow ratio ϕ is expressible in terms of ν, the ratio of the number N_L of open channels in any given assembly to the number N_r in the reference assembly:

$$\phi=(L/3\text{ cm})(N_r/N_L), \tag{A9}$$

and

$$\nu=\frac{N_L}{N_r}=\frac{L/(3\text{ cm})}{\phi}. \tag{A10}$$

In this limit, N_r must be replaced by N_L in Eq. (A5) for the corrected values (K_{expt}''):

$$K_{\text{expt}}''=K_{\text{expt}}(N_r/N_L)=K_{\text{expt}}/\nu. \tag{A11}$$

Since K_{th} is not dependent on N, K_{expt}'' must be compared with the original reference curve K_r (Fig. 5), and

thus

$$\kappa_n=\frac{K_{\text{expt}}''}{K_r}=\frac{K_{\text{expt}}/\nu}{K_r}=\frac{\kappa}{\nu}, \tag{A12}$$

but from Eqs. (A4) and (A10), $\alpha^2=\nu$, and so

$$\kappa_n=\kappa_a=\kappa', \tag{A13}$$

where κ' is the ratio given in line 8 of Table II.

Note added in proof. The assumption of incompressible gas flow with zero slip is implicit in Eq. (A1). In analyzing the relative gas-flow measurements, the validity of this assumption does not affect the evaluation of κ_n; approximate calculations for κ_a show that the inclusion of slip corrections does not appear to eliminate the "length effect."

PHYSICAL REVIEW VOLUME 139, NUMBER 6A 13 SEPTEMBER 1965

Position- and Time-Dependent Diffusion Modes for Electrons in Gases

JAMES H. PARKER, JR.
Westinghouse Research Laboratories, Pittsburgh, Pennsylvania
(Received 16 April 1965)

The pure-diffusion (field-free) distribution function for electrons in a gas enclosed by absorbing walls is obtained. The distribution is described in terms of spatial modes, each of which decays exponentially with time. Special emphasis is placed on the lowest modes which explicitly display the "diffusion cooling" effect for electrons.

I. INTRODUCTION

THIS paper deals with the pure-diffusion (field-free) energy distributions for electrons in a gas and enclosed by absorbing walls. The present study is an extension of previous work[1] by the author on the spatial dependence of distribution functions for electrons in the presence of electric fields. The purpose of the present work is to describe the manner in which the distribution function for electrons, which are initially *not* in thermal equilibrium with the gas, changes with time and position owing to collisions between the electrons and the gas atoms and to diffusion of the electrons to the walls. This descritpion is given in terms of spatial modes, each of which decays exponentially with time. It will be shown that in general the electrons never come into equilibrium with the gas but have a terminal energy that is lower than the thermal energy of the gas. This effect, which has been called "diffusion cooling,[2]" is displayed by the lowest modes, i.e., the modes with the longest decay times. For simplicity the interaction between the electrons and atoms is taken as elastic and only the plane-parallel geometry is considered. The entire mode system is given for the case of an energy-independent collision frequency while only the lowest modes are obtained for the case of an energy-independent collision cross section.

II. CONSTANT COLLISION FREQUENCY

The starting point for the present discussion is the Boltzmann equations for $f^0(\mathbf{r},v,t)$ and $\mathbf{f}^1(\mathbf{r},v,t)$. These functions represent, respectively, the isotropic and nonisotropic parts of the electron distribution function, i.e.,

$$f(\mathbf{r},\mathbf{v},t)=f^0(\mathbf{r},v,t)+\mathbf{f}^1(\mathbf{r},v,t)\cdot\hat{v}$$

where $\mathbf{r}$ is the position vector and $\mathbf{v}$ is the electron velocity. The Boltzmann equations for f^0 and $\mathbf{f}^1$, with the collision frequency independent of energy, are[3]

$$\frac{\partial f^0}{\partial t}=\frac{2m\nu}{M\epsilon^{1/2}}\frac{\partial}{\partial\epsilon}\left[\epsilon^{3/2}\left(f^0+kT\frac{\partial f^0}{\partial\epsilon}\right)\right]-\frac{1}{3}\left(\frac{2\epsilon}{m}\right)^{1/2}\nabla_r\cdot\mathbf{f}^1, \tag{1}$$

and

$$\frac{\partial\mathbf{f}^1}{\partial t}+\nu\mathbf{f}^1=-\left(\frac{2\epsilon}{m}\right)^{1/2}\nabla_r f^0, \tag{2}$$

where m is the electron mass, M the atomic mass, ϵ the electron kinetic energy, ν the momentum-transfer collision frequency, and T the gas temperature. It will be assumed that f^0 varies sufficiently slowly so that Eq. (2) can be written as

$$\nu\mathbf{f}^1\approx-(2\epsilon/m)^{1/2}\nabla_r f^0. \tag{3}$$

The conditions under which this approximation is valid will be discussed at the end of this section. When Eq. (3) is combined with Eq. (1), the resulting equation for f^0 is

$$\epsilon^{-3/2}\frac{\partial}{\partial\epsilon}\left[\epsilon^{3/2}\left(f^0+kT\frac{\partial f^0}{\partial\epsilon}\right)\right]+\frac{M}{3m^2\nu^2}\nabla_r^2 f^0=\frac{M}{2m\nu\epsilon}\frac{\partial f^0}{\partial t}. \tag{4}$$

[1] J. H. Parker, Jr., Phys. Rev. **132**, 2096 (1963).
[2] M. A. Biondi, Phys. Rev. **93**, 1136 (1954).
[3] The detailed derivation of these equations along with a discussion of the approximations used in obtaining them is given by W. P. Allis, in *Handbuch der Physik*, edited by S. Flügge (Springer-Verlag, Berlin, 1956), Vol. 21. Also see T. Holstein, Phys. Rev. **70**, 367 (1946).

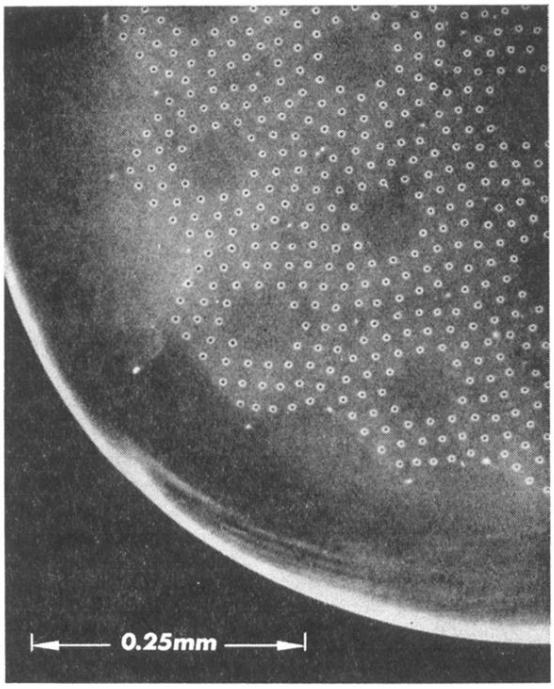

FIG. 1. Microphotograph (one-quarter view) of the end of a fiber bundle. The small dark spots are the capillary orifices. The light annular regions are the capillary walls and the darker region surrounding them is the embedding glass matrix. The outer boundary of the glass matrix is circular in cross section (diameter $\simeq$1.0 mm).